

## 20. MINERALIZATION AND TRACE ELEMENT VARIATION IN DEEP-SEA PELAGIC SEDIMENTS OF THE WHARTON BASIN, INDIAN OCEAN

Anthony C. Pimm, Scripps Institution of Oceanography, La Jolla, California

### INTRODUCTION

Several features of the cores recovered from Leg 22 indicated varying degrees and kinds of mineralization in pelagic sediments. The nature of this mineralization could not be resolved by the routine microscopic examination of smear slides onboard the ship. It was therefore decided to use analytical methods to investigate vertical variations in the chemical composition of the three sites (211, 212, 213) drilled in the Wharton Basin (Figure 1). In particular, the main features of interest which were to be investigated included:

- 1) basal iron-oxide facies (Sites 211, 212, 213)
- 2) possible effects of intrusion of sill (Site 211)
- 3) chemistry of reduced zones in clay adjacent to chalk units (Site 212)
- 4) dark banding in siliceous oozes (Site 213)
- 5) trace element composition of typical brown clays (Sites 211, 212, 213).

### METHODS OF INVESTIGATION

Using the visual core descriptions made onboard ship, 58 samples were selected for a rapid reconnaissance study using the X-ray fluorescence technique of Fitzgerald and Gantzel (1971). Photographs of the energy dispersion spectra for each sample were compared with U.S.G.S. standard W1, and a semiquantitative estimate of the relative abundance of various elements was made by directly comparing the peak heights. For the analysis of Fe and Mn the samples were counted for 100-sec intervals, but for the trace elements counts over 30-min intervals were necessary. Photographs of all the energy dispersion spectra obtained during this study are stored with the Curator of the Deep Sea Drilling Project, La Jolla, California.

Based on the results of this preliminary study, 28 of the original 58 samples, which showed higher values (compared with W1) of one or more elements (Table 1), were prepared for atomic absorption analysis. This analysis was carried out on a Perkin-Elmer 403 Atomic Absorption Spectrophotometer using the digital concentration readout. For Ni, Cu, Pb, Zn, Mn, Fe, and Cr an air-acetylene flame was used with the standard burner head (4 in, single slot); for V and Ti a nitrous-oxide acetylene flame was used with the nitrous-oxide burner head (5 cm, single slot). Suggested Perkin-Elmer standard conditions and instrument settings were followed, except that the burner head was set perpendicular to the light path in the analysis for Mn and Fe because of the high sensitivity of the instrument to these elements. Also, the Perkin-Elmer Deuterium-Arc background corrector was used in the Ni determination.

All dried and ground samples were weighed to 0.5 g, placed in Teflon decomposition bombs, and wetted with distilled water. Approximately 1 ml of concentrated aqua (3 HCl:1 HNO<sub>3</sub>) was added to the samples, and then 6 ml of concentrated HF was added. The vessels were then tightly covered and placed in the oven for 1 hr at 110°C. When cooled, samples were transferred to 50-ml polyethylene volumetric flasks and diluted to the mark with a solution of distilled water and ~2.2 g boric acid. The solutions were then mixed and stored in polyethylene bottles.

Standards were prepared from commercial 1000 ppm solutions to the following concentrations:

Cr	2.0, 1.0, 0.5 ppm	Pb	5, 2, 1 ppm
V	2.0, 1.0, 0.5 ppm	Zn	2.0, 1.0, 0.5 ppm
Ti	100, 50, 10 ppm	Mn	100, 50, 10 ppm
Ni	10, 5, 4, 2, 1 ppm	Fe	100, 50, 10 ppm
Cu	5, 2, 1 ppm		

A set of U.S.G.S. standards was prepared and analyzed using the same instrument setup and method of preparation as for the samples. The values obtained agreed with the reported range of values for the U.S.G.S. standards, with one exception. The nickel values obtained were much higher than the reported range of values, but when the D<sub>2</sub> background corrector was used the results were within the reported range. Hence, it was concluded that the D<sub>2</sub> background corrector removed interferences for Ni, and the sediment samples were rerun using this corrector. The element concentration values obtained and the reported range of values for the U.S.G.S. standards W1, G2, and BCR-1 are given in Table 2.

Ranges of error are recorded in Table 2 for each element. The error was determined by choosing random, duplicate samples and weighing, decomposing, and analyzing these samples along with the others and by comparing the difference between duplicate samples.

### RESULTS AND DISCUSSION

The results of the reconnaissance semiquantitative analysis are given in Table 1 and of the detailed quantitative analysis of some of these same samples in Table 2. Most of the samples in the latter analysis are from Sites 212 and 213, and downhole plots of the results against lithology are shown in Figures 2 and 3, respectively.

In addition, some further analytical results were generously made available by R. Hekinian. These are major element analysis of nine sediment samples selected from Sites 211, 212, and 213 (Table 3) and trace element analysis of four igneous rock samples from Sites 211 and 213 (Table 4).

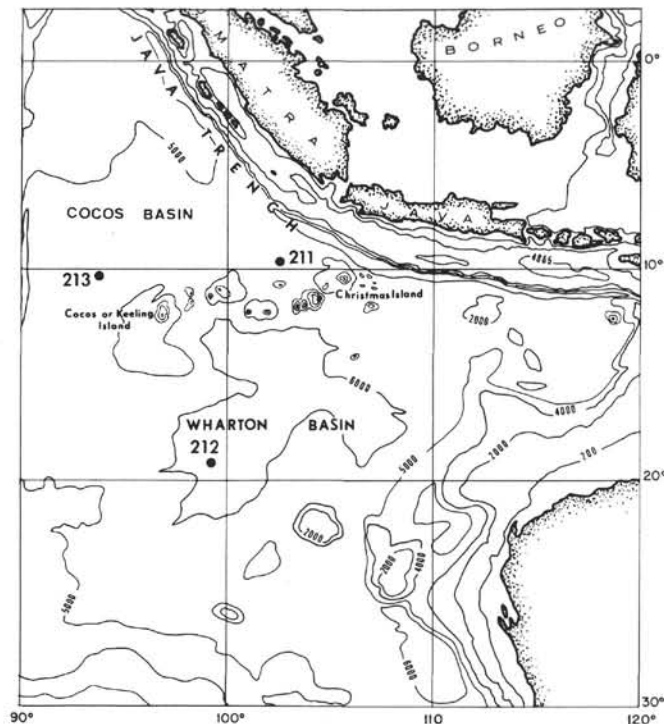


Figure 1. Location of DSDP Leg 22 sites in Wharton Basin.

### Basal Iron-Oxide Facies

Many sites drilled during the course of the Deep Sea Drilling Project have shown the presence of an iron-oxide-enriched sediment facies at the base of the sediment column immediately overlying basalts, which were presumed to have been generated from a mid-oceanic ridge-type spreading center. Descriptions of these iron-rich facies have been given by Peterson et al. (1970, p. 421), von der Broch and Rex (1970), von der Borch et al. (1971), Drever (1971), Lancelot et al. (1972, pp. 911-916), and Cronan (1973).

The iron-oxide-rich facies in Leg 22 sites was recognized on the basis of color and an abundance of iron-oxide-rich clayey aggregates and high relief grains seen in smear slides. Visual estimates show that the iron-oxide-rich clayey aggregates make up at least 15% and may range as high as 80% in places of the sediment. At Sites 212 and 213 the iron-oxide facies is about 30 and 40 meters thick, respectively (Figures 2 and 3). However, the analyses show that only the lowermost sample (probably within 5 meters of the basalt) in each site contained more than 10% total iron. Samples higher in this facies did not contain significantly greater (i.e., more than double) amounts of total iron normally present in more typical pelagic brown clays much higher in the succession.

Major element analyses (Table 3) confirm the existence of an iron-rich basal facies at Site 212, Core 38 and Site 213, Core 16. It should be noted that if the analyses were recalculated on a dry weight basis, the  $Fe_2O_3$  content would be higher than that shown in Table 3. The  $Fe_2O_3$  major element and Fe element analyses made by different laboratories and techniques show a good agreement: for example, the higher iron content at Site 213 than 212 and

TABLE 1  
Semiquantitative X-Ray Fluorescence Analyses

Lab P. No.	Core, Section, Interval (cm)	Ni	Cu	Zn	Pb	Mn	Fe	Other Elements
<b>Site 211</b>								
1	1-1,14-16	+	=	+	=	+	-	
2	10-CC	+	=	+	=	-	=	
3	11-CC	=	=	+	=	-	=	
4	11-CC	-	-	+	=	-	-	
5	12-1,11-13	=	=	+	=	-	-	
6	12-2,122-124	+	-	=	=	-	-	
7	12-2,136-138	-	-	+	=	-	-	
8	13-1,68-69	=	=	+	=	-	=	
9	13-1,69-70	=	=	+	=	-	-	
10	13-1,138-139	=	=	+	=	-	-	
11	14-1,18-20	=	=	+	=	-	-	
12	14-1,28-30	=	=	+	=	-	-	
13	14-1,61-63	=	-	=	=	-	-	
14	15-1,118-120	=	=	+	=	-	+	Zr+ Sr+
<b>Site 212</b>								
15	2-1,114-116	+	+	+	=	+	+	
16	2-3,111-113	+	+	+	=	+	-	
17	4-1,122-123	+	=	+	++	+	-	
18	10-1,32-33	+	+	+	+	+	-	
19	10-2,84-86	-	-	=	=	-	-	Sr+
20	10-4,79-80	=	-	=	=	-	-	Sr+
21	15-1,63	++	++	=	=	-	=	Rb+ Sr=
22	15-1,67-68	+	+	+	+	-	+	Sr=
23	15-1,97-100	+	+	+	++	+	+	Sr=
24	16-2,	+	+	+	+	+	+	
25	18-2,5-6	+	=	+	+	+	+	
26	23-5,105-107	=	++	+	-	-	-	
27	26-2,81-82	-	-	+	=	-	-	Sr+
28	27-1,102-104	=	=	+	++	-	-	Sr=
29	27-1,128-130	++	+	+	++	-	-	Rb+
30	27-4,31-32	=	+	+	+	-	-	
31	27-6,66-68	=	=	+	=	-	-	
32	28-1,55-57	=	=	+	=	-	-	Cr=
33	28-1,61	+	+	+	=	-	-	
34	29-1,57	=	=	+	=	-	-	Cr+
35	29-1,71	+	+	+	+	-	-	
36	35-3,80-82	=	=	=	=	-	-	Sr+
37	35-4,80-82	=	=	+	=	-	-	Sr+
38	35-5,10-12	=	+	+	=	-	-	Sr= Cr=
39	35-5,40-42	=	+	+	=	-	-	Cr=
40	36-1,107-108	+	-	+	=	-	-	
41	37-1,108-110	+	+	+	=	-	-	
42	38-1,73-74	+	+	+	-	-	-	
43	38-2,7	+	-	+	=	-	+	Zr= Cr+ Ti++
44	38-2,14	+	+	+	+	-	-	
45	38-2,31	+	-	=	+	+	+	
<b>Site 213</b>								
46	1-1,5-7	+	++	+	=	-	-	Br+
47	1-1,70-72	+	+	+	=	-	-	Br+
48	2-5,49-51	+	+	+	=	-	-	Br+
49	3-1,30-32	+	+	+	=	-	-	Br+
50	3-6,19-21	++	++	+	++	++	-	Cr++
51	8-3,10-12	+	+	+	=	-	-	
52	8-6,140-142	+	+	+	=	-	-	
53	9-6,80-82	+	+	+	=	-	-	
54	10-3,70-72	+	+	+	=	-	-	
55	11-4,72-74	++	+	=	+	+	-	
56	13-3,80-81	+	+	+	+	+	+	
57	14-2,70-72	+	+	+	-	-	-	
58	16-4,145-147	+	+	+	+	++	+	

Note: Value compared to U.S.G.S. standard W1; semiquantitative symbols used in table: - not detected, = same as W1; + higher than W1; ++ much higher than W1.

the low iron contents at Site 211 and in Core 37 at Site 212.

A comparison of the Mn and trace element content in Table 2 with other analytical results reported by Drever (1971, p. 966), Cronan (1973, p. 603), and Bostrom et al. (1969), shows there is no consistent enrichment of these elements in every instance, though some enrichment of one or other trace elements is apparent if the total iron content is particularly high. So far as Sites 212 and 213 are concerned, the only possible enrichment of another element in the most iron-rich zone is the higher Zn value at Site 212. All other element values in the basal iron-oxide facies are comparable with those of more typical deep-sea clays higher in the sedimentary column.

At Site 213 the iron enrichment is restricted to clay beds, and the interbeds of calcareous ooze show no more visually detectable iron oxide than is typical for such material. At Site 212 slightly metamorphosed limestone trapped between basalt pillows shows no iron enrichment. At Site 211 clayey calcareous ooze was recovered from a 16-meter interval (Cores 12-14) between basaltic basement and a sill (see Chapter 2), and this sediment shows a pronounced reddish to orange brown fine banding on a 1-5 mm scale. However, two samples analyzed from this interval showed no evidence of any mineralization; even the sample (Core 12) taken from the dusky red zone immediately below the sill was not enriched in iron.

The K<sub>2</sub>O content in this zone is particularly high (Table 3) and may be genetically linked to the relatively high K<sub>2</sub>O content in the diabase sill compared with the other basalts at Sites 211, 212, and 213 (Hekinian, Chapter 17).

All the authors listed previously who have described basal iron-oxide facies in DSDP cores have attributed their origin to volcanic hydrothermal exhalations following the Bostrom and Peterson (1966) model for the East Pacific Rise. A similar explanation is invoked for this facies in the Leg 22 sites.

The absence of significant iron enrichment in the calcareous sediments at the base of Site 211, in the metamorphosed limestone between basalt pillows at Site 212, and in interbeds of calcareous ooze at Site 213 supports the hypothesis that the ferruginous material in the clay beds is syngenetic with the sediment and thus has not been introduced by permeation from below. Also, if the original source of the iron was in the basalts, a depletion of Fe might be expected in the latter. The analyses of igneous rocks given in Table 4 certainly do not show evidence of such a depletion. However, so few analyses may not be conclusive because Corliss (1970) has pointed out that a depletion of Fe, Mn, Co, and rare earth elements only occurs in the holocrystalline interiors of submarine flows relative to the rapidly cooled margins. The two samples analyzed from Site 213 did, however, come from the fresher phaneritic portion of pillow lavas (see Hekinian, Chapter 17, fig. 2). The sample from the diabase in Site 211 came from the center of the sill, but that from the amphibolite in Core 15 of Site 211 was from the aphanitic zone. In all instances, though, the iron content is remarkably uniform. This provides strong support to the argument that the iron of the basal sediment facies has not been derived directly from the closely associated volcanic rocks.

### Contact Zones Between Chalk and Clay in Site 212

One sample from each of the three reduced grayish blue-olive green clay intervals adjacent to chalk units in Site 212 was analyzed (Cores 15-1, 23-5, 27-1 in Table 2). Details of the stratigraphic sequence of each sample can be seen on the core forms given in the site report (Chapter 3). These clays show very low Mn values, but no other characteristics are common to all three. Most striking is the high nickel content of 2730 ppm in one sample, and associated with this are slightly higher Cu and Pb values.

In addition to the sample in the reduced zone in Core 15, a sample was also analyzed from the more typical brown clay 34 cm below. Comparing the two analyses, the reduced zone is depleted in Fe and Mn and enriched in Cr, Cu, Ni, Pb, and V.

### Dark Brown Mn-rich Layers in Site 213

Cores 3 through 6 recovered from 18 to 50 meters below the sea floor at Site 213 contain common thin layers of dark to very dark brown intervals within the diatom ooze sequence. These layers are mostly in the 10 to 30 cm thickness range and are described on the core forms in the site report (Chapter 4) as Mn-Fe-rich layers. The analysis of one sample from such a layer in Core 3 compared with two other samples of siliceous ooze from Cores 1 and 2 confirms that these layers are very rich in Mn—nearly 8% compared to <1%. The iron content is, however, lower than usual, as is the Ti value. Along with the high Mn, considerable enrichment of Cu and V is evident (Table 2 and Figure 2).

### Variation Downhole of Fe, Mn, and Trace Elements

With the exception of the samples taken in unusual sediment types for the specific studies mentioned above, the brown clays analyzed show very little variation in the relative proportions of the trace elements and Fe and Mn contents downhole. Typical ranges of values for the three sites (in ppm) are:

Site	Cr	Cu	Ni	Pb	Ti
211	40-50	100-300	100-150	50	6000-7000
212	50-90	100-400	100-400	30-100	6000-8000
213	35-60	200-500	100-500	30-70	3500-6000

Site	V	Zn	Fe	Mn
211	200-300	150-160	4.0-7.0	<1
212	200-350	150-200	4.5-8.5	<2
213	150-250	100-200	3.0-7.0	<2

### ACKNOWLEDGMENTS

The X-ray fluorescence and atomic absorption analyses were carried out in the Scripps Institution of Oceanography analytical facility under the supervision of R. Laborde. The author would also like to extend his appreciation to R. Fitzgerald for time on the X-ray fluorescence unit used in this study. Particular thanks are extended to M. Sangstrom who prepared all samples and also operated the atomic absorption unit.

TABLE 2  
Atomic Absorption Analyses<sup>a</sup>

Lab No. P	Site, Core, Interval (cm)	Cr	Cu	Fe	Mn	Ni	Pb	Ti	V	Zn	Visual Core Description
<b>Site 211</b>											
1	1-1,14-16	44	302	40,500	10,900	150	47	6,200	216	157	Dark yellowish brown diatom-rich clay
2	10-CC	51	123	72,500	602	130	51	6,800	311	155	Moderate brown and dusky yellowish brown clay
6	12-2, 122-124	65	44	48,500	2,630	100	24	8,280	146	107	Dusky red nanno-rich clay adjacent to sill
12	14-1,28-30	77	86	52,000	950	30	19	9,400	154	131	Moderate brown nanno-rich clay 35 cm above basalt
<b>Site 212</b>											
15	2-1,114-116	86	378	59,500	10,900	250	59	7,400	284	148	Moderate brown clay with iron-oxide aggregates
17	4-1,122-123	81	158	67,000	12,000	230	95	5,960	264	154	Mixed nanno ooze and clay
18	10-1,32-33	84	369	86,000	17,300	320	79	6,480	285	176	Dark brown iron-oxide-rich clay
21	15-1,63	108	868	53,000	628	2,730	118	7,150	495	134	Grayish blue green claystone mineralized (contact zone below chalk)
23	15-1,97-100	78	424	80,500	21,900	390	85	7,060	337	172	Iron-oxide clay
24	16-2, shaving	91	358	79,000	18,100	31	76	7,430	330	184	Dusky brown iron-oxide claystone
25	18-2,5-6	60	221	80,500	15,500	185	63	6,400	313	175	Dusky brown iron-oxide claystone
26	23-5,105-107	52	168	68,000	1,260	65	13	5,170	203	162	Grayish olive green zeolite-rich clay (contact zone below chalk)
29	27-1,128-130	68	505	42,000	485	460	56	7,330	389	334	Medium bluish gray (reduced zone 50 cm below contact zone)
33	28-1,61	61	164	67,000	4,320	140	46	6,430	339	189	Dark yellowish brown clay
35	25-1,71	70	217	75,000	3,610	120	48	8,650	263	211	Dark yellowish brown clay
40	36-1,107-108	78	119	59,500	9,370	140	33	7,260	214	177	Moderate yellowish-brown claystone
41	37-1,108-110	47	163	44,000	9,180	140	12	6,200	184	153	Moderate reddish brown with brown banding
44	38-2,14	73	347	11,000	3,270	150	12	7,180	348	210	Grayish brown clay
<b>Site 213</b>											
46	1-1, 5-7	36	292	34,000	6,430	130	39	3,600	162	116	Medium brown clay siliceous ooze
48	2-5,49-51	45	232	39,500	1,140	130	31	4,550	173	108	Light brown reddish yellow clay siliceous ooze
50	3-6, 19-21	33	1,046	20,100	78,200	290	214	2,490	675	108	Very dark brown manganese-rich diatom ooze
52	8-6,140-142	47	466	47,500	9,500	260	60	4,650	225	140	Dark brown clay
53	9-6,80-82	36	480	44,000	12,800	240	55	4,000	188	148	Dark brown clay
54	10-3,70-72	35	466	45,000	13,900	280	52	4,080	194	137	Dark brown clay
55	11-4,72-74	57	490	59,500	21,400	500	70	5,050	238	175	Dusky yellowish brown clay (zeolite-rich)
56	13-3,80-81	39	346	64,000	18,400	420	54	6,040	257	201	Dusky brown iron-oxide-rich clay
57	14-2,70-72	50	228	70,500	11,400	210	61	6,270	244	194	Moderate brown iron-oxide-rich clay
58	16-4,145-147	39	523	162,000	32,000	280	168	5,000	713	350	Grayish brown clay-rich iron oxide
<b>Error</b>		±2%	±2%	±2%	±3%	±5% <sup>b</sup>	±2% <sup>c</sup>	±7%	±2%	±2%	
<b>U.S.G.S. Standards</b>											
W1	found	118	121	73,500	1,550	56	11	8,500	240	94	
	range	90-160	80-150	77,200	1,310	55-88	5-10	6,300	120-320	20-95	
G2	found	12	12	19,500	286		35	3,500	53	90	
	range	5-29	2-17	18,100	250		15-43	3,000	26-60	42-138	
BCR-1	found	16	18	87,100	1,410		18	16,500	136	136	
	range	8-45	7-33	89,800	1,375		4-35	13,000	120-700	94 278	

<sup>a</sup>All values in ppm.

<sup>b</sup>Except for values less than 200 ppm, perhaps ±10%.

<sup>c</sup>Except for values less than 20 ppm.

## REFERENCES

- Bostrom, K. and Peterson, M. N. A., 1966. Precipitates from hydrothermal exhalations on the East Pacific Rise: *Econ. Geol.*, v. 61, p. 1258.
- Bostrom, K., Peterson, M. N. A., Joensuu, O., and Fisher, D., 1969. Aluminum poor ferromanganoan sediments on active oceanic ridges: *J. Geophys. Res.*, v. 74, p. 3261.
- Corliss, J. B., 1970. Mid-ocean ridge basalts: Ph.D. thesis, University of California, San Diego.
- Cronan, D. S., 1973. Basal ferruginous sediments cored during Leg 16, Deep Sea Drilling Project. *In* Initial Reports of the Deep Sea Drilling Project, Volume XVI: Washington (U. S. Government Printing Office), p. 601-604.
- Drever, J. I., 1971. Chemical and mineralogical studies, Site 66. *In* Initial Reports of the Deep Sea Drilling Project, Volume VII: Washington (U. S. Government Printing Office), p. 965-975.
- Fitzgerlad, R. and Gantzel, P., 1971. X-ray energy spectrometry in the 0.1 to 10 Å range. *In* Energy dispersion X-ray analysis: X-ray and electron probe analysis: Am. Soc. Testing Materials, STP 485, p. 3-35.
- Lancelot, Y., Hathaway, J. C., and Hollister, C. D., 1972. Lithology of sediments from the western North Atlantic, Leg 11 Deep Sea Drilling Project. *In* Initial Reports of the Deep Sea Drilling Project, Volume XI: Washington (U. S. Government Printing Office), p. 901-949.
- Peterson, M. N. A., Edgar, N. T., von der Borch, C. C., and Rex, R. W., 1970. Cruise leg summary and discussion. *In* Initial Reports of the Deep Sea Drilling Project, Volume II: Washington (U. S. Government Printing Office), p. 413-427.
- von der Borch, C. C. and Rex, R. W., 1970. Amorphous iron oxide precipitates in sediments cored during Leg 5, Deep Sea Drilling Project. *In* Initial Reports of the Deep Sea Drilling Project, Volume V: Washington (U. S. Government Printing Office), p. 541.
- von der Borch, C. C., Nesteroff, W. D., and Galehouse, J. S., 1971. Iron-rich sediments cored during Leg 8 of the Deep Sea Drilling Project.

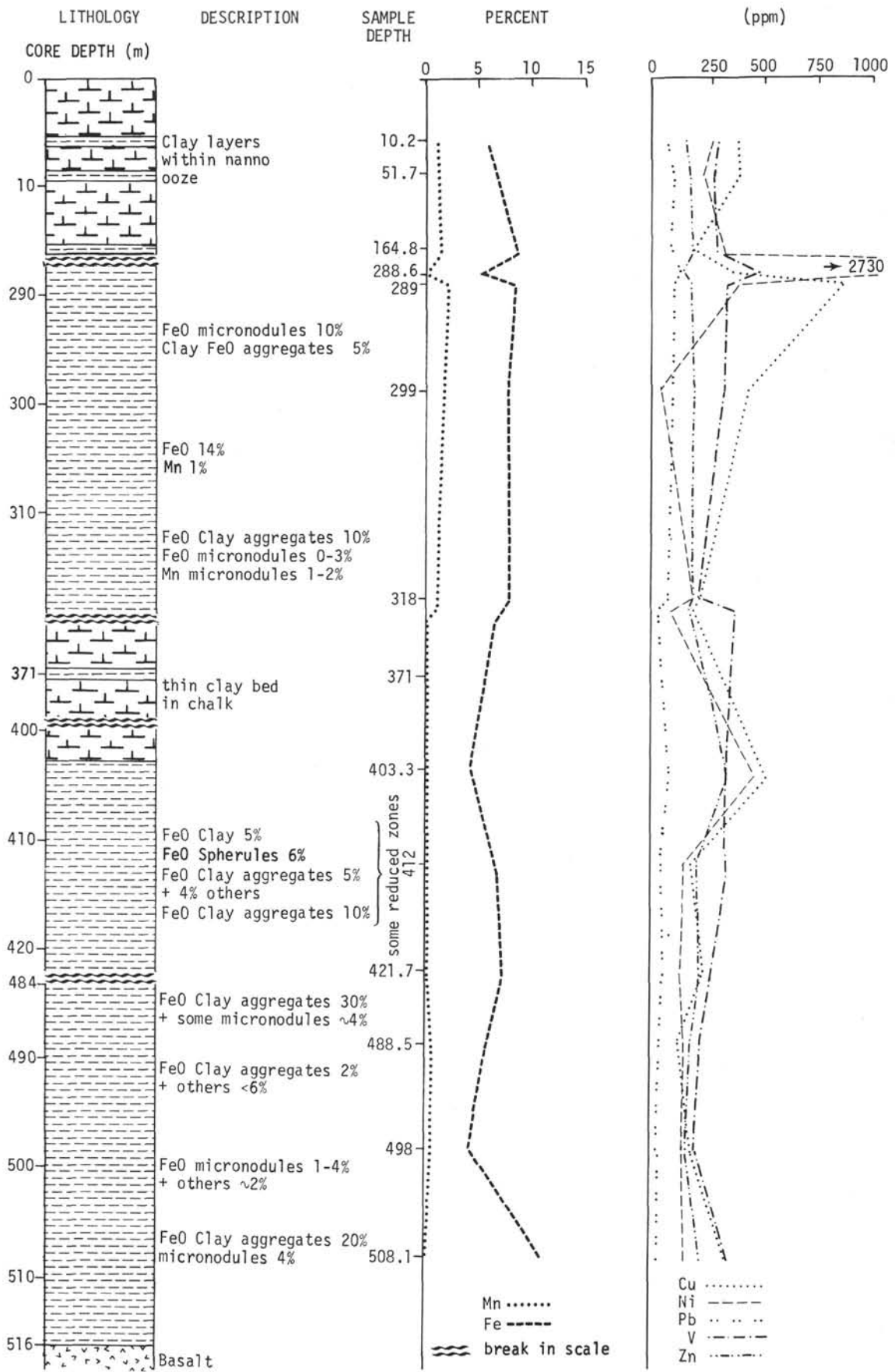


Figure 2. Elemental variation downhole in Site 212.

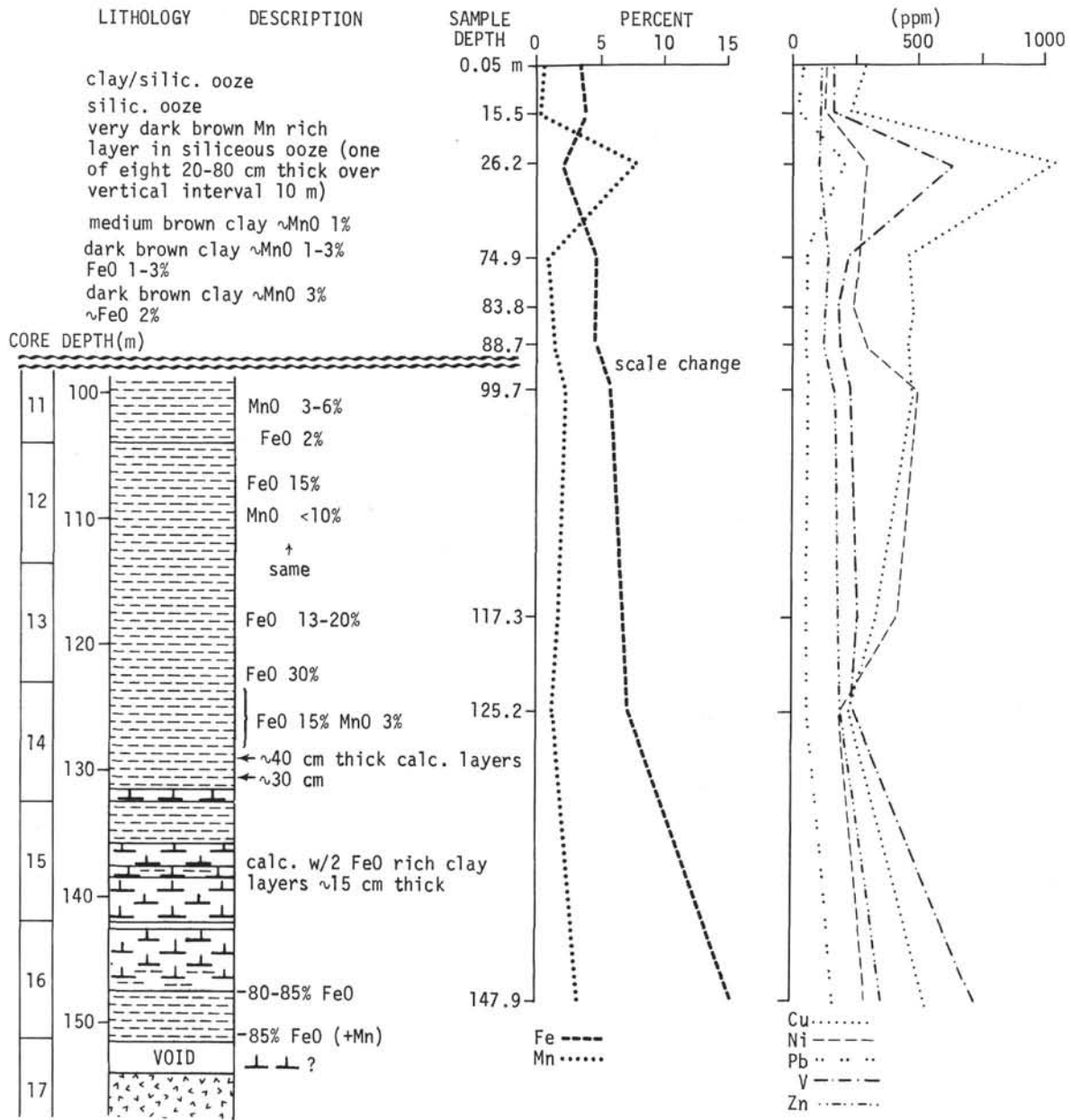


Figure 3. Elemental variation downhole in Site 213.

TABLE 3  
Major Element X-Ray Fluorescence Analyses of Sediments<sup>a</sup>

Core, Section, Depth in Core (cm)	SiO <sub>2</sub>	Al <sub>2</sub> O <sub>3</sub>	Fe <sub>2</sub> O <sub>3</sub>	MgO	CaO	Na <sub>2</sub> O	K <sub>2</sub> O	TiO <sub>2</sub>	P <sub>2</sub> O <sub>5</sub>	Ignition (CO <sub>2</sub> + H <sub>2</sub> O)
<b>Site 211</b>										
12-2,124-128	46.15	12.47	6.79	2.16	9.00	—	7.53	0.90	0.27	13.49
14-1,65	44.36	11.30	6.94	3.71	7.84	1.47	3.62	0.99	0.25	18.30
<b>Site 212</b>										
18-1,105-107	41.70	15.21	10.84	2.49	0.77	—	2.04	0.70	0.36	22.59
35-5,44-45	47.12	16.08	10.44	2.96	0.66	—	2.68	0.71	0.25	17.90
37-1 90 91	54.73	13.15	6.84	3.31	0.88	—	2.96	0.72	0.29	16.24
38-2 98	45.50	11.85	14.69	3.26	0.94	1.41	3.47	0.87	0.38	14.32
<b>Site 213</b>										
9-6 84 85	44.92	13.83	5.94	3.60	1.32	—	1.62	0.46	0.53	19.96
16-4,138-139	38.39	8.86	19.57	3.48	4.19	—	2.49	0.56	1.14	19.92

<sup>a</sup>Analysis by P. Cambon, Centre Oceanologique de Bretagne, Brest, France. All values given in percent.

TABLE 4  
Trace Element Analysis of Igneous Rock Samples

Core, Section, Depth in Core (cm)	Ti	V	Cr	Fe	Co	Ni	Cu	Zn	Rock Type
<b>Site 211</b>									
15-2,0-5	15,100	115	75	63,600	55	110	21	70	Amphibolite
12-1,143-145	13,280	140	275	73,800	65	155	31	80	Diabase
<b>Site 213</b>									
18-2,101-103	6,060	235	280	74,000	90	135	80	75	Basalt
18-1,144-150	6,180	235	380	73,800	90	115	80	85	Basalt

Note: Values given in ppm.